Notes on Numerical Fluid Mechanics
and Multidisciplinary Design 124

Andreas Dillmann · Gerd Heller
Ewald Krämer · Hans-Peter Kreplin
Wolfgang Nitsche · Ulrich Rist *Editors*

New Results in Numerical and Experimental Fluid Mechanics IX

Contributions to the 18th STAB/DGLR Symposium, Stuttgart, Germany, 2012

Springer

Notes on Numerical Fluid Mechanics and Multidisciplinary Design

Volume 124

About this Series

Notes on Numerical Fluid Mechanics and Multidisciplinary Design publishes state-of-art methods (including high performance methods) for numerical fluid mechanics, numerical simulation and multidisciplinary design optimization. The series includes proceedings of specialized conferences and workshops, as well as relevant project reports and monographs.

Andreas Dillmann · Gerd Heller
Ewald Krämer · Hans-Peter Kreplin
Wolfgang Nitsche · Ulrich Rist
Editors

New Results in Numerical and Experimental Fluid Mechanics IX

Contributions to the 18th STAB/DGLR Symposium, Stuttgart, Germany, 2012

Springer

Editors
Andreas Dillmann
Hans-Peter Kreplin
Deutsches Zentrum für Luft- und Raumfahrt (DLR)
Institut für Aerodynamik und Strömungstechnik
Göttingen
Germany

Gerd Heller
Airbus Deutschland
Bremen
Germany

Ewald Krämer
Ulrich Rist
Institut für Aerodynamik und Gasdynamik
University of Stuttgart
Stuttgart
Germany

Wolfgang Nitsche
Institut für Luft- und Raumfahrt
TU Berlin
Berlin
Germany

ISSN 1612-2909 ISSN 1860-0824 (electronic)
ISBN 978-3-319-03157-6 ISBN 978-3-319-03158-3 (eBook)
DOI 10.1007/978-3-319-03158-3
Springer Cham Heidelberg New York Dordrecht London

Library of Congress Control Number: 2013957123

Printed on acid-free paper

Springer is part of Springer Science+Business Media (www.springer.com)

Preface

This volume contains the papers presented at the 18th DGLR/STAB-Symposium held in Stuttgart, Germany, in November, 6–7, 2012 and organized by the Institute of Aerodynamics and Gas Dynamics of Stuttgart University. STAB is the German Aerospace Aerodynamics Association, founded toward the end of the 1970s, whereas DGLR is the German Society for Aeronautics and Astronautics (Deutsche Gesellschaft für Luft- und Raumfahrt—Lilienthal Oberth e.V.).

The mission of STAB is to foster development and acceptance of the discipline "Aerodynamics" in Germany. One of its general guidelines is to concentrate resources and know-how in the involved institutions and to avoid duplication in research work as much as possible. Nowadays, this is more necessary than ever. The experience made in the past makes it easier now, to obtain new knowledge for solving today's and tomorrow's problems. STAB unites German scientists and engineers from universities, research-establishments, and industry doing research and project work in numerical and experimental fluid mechanics and aerodynamics for aerospace and other applications. This has always been the basis of numerous common research activities sponsored by different funding agencies.

Since 1986 the symposium has taken place at different locations in Germany every 2 years. In between STAB workshops regularly take place at the DLR in Göttingen. The changing meeting places were established as focal points in Germany's Aerospace Fluid Mechanics Community for a continuous exchange of scientific results and their discussion. Moreover, they are a forum where new research activities can be presented, often resulting in new commonly organized research and technology projects.

It is the ninth time now that the contributions to the Symposium are published after being subjected to a peer review. The material highlights the key items of integrated research and development based on fruitful collaboration of industry, research establishments, and universities. The research areas include airplane aerodynamics, multidisciplinary optimization and new configurations, turbulence research and modeling, laminar flow control and transition, rotorcraft

aerodynamics, aeroelasticity and structural dynamics, numerical simulation, experimental simulation and test techniques, aeroacoustics as well as the rather new fields of biomedical flows, convective flows as well as aerodynamics and acoustics of ground vehicles.

From some 90 lectures presented at the Symposium 68 are included in this book.

The Review Board, partly identical with the Program Committee, consisted of J. Arnold (Göttingen), K. Becker (Bremen), S. Becker (Erlangen), M. Behr (Aachen), H. Bieler (Bremen), P. Birken (Kassel), J. Bosbach (Göttingen), C. Breitsamter (Garching), G. Brenner (Clausthal), M. Buschmann (Dresden), C. Cierpka (Neubiberg), K. Ehrenfried (Göttingen), J. Fassbender (Bremen), D. Fiala (Stuttgart), H. Foysi (Siegen), A. Friedl (Neubiberg), J. Fröhlich (Dresden), A. Gardner (Göttingen), N. Gauger (Aachen), K. Geurts (Aachen), C. Gmelin (Berlin), P. Gnemmi (St. Louis), C. Grabe (Göttingen), S. Grundmann (Darmstadt), S. Guerin (Berlin), H. Hansen (Bremen), R. Hartmann (Braunschweig), A. Hartmann (Aachen), M. Haupt (Braunschweig), S. Hein (Göttingen), R. Heinrich (Braunschweig), M. Hepperle (Braunschweig), H. Herwig (Hamburg), S. Hickel (Garching), R. Höld (Unterschleißheim), R. Hörnschemeyer (Aachen), S. Illi (Stuttgart), T. Indinger (Garching), S. Jakirlic (Darmstadt), L. Jehring (Cottbus), J. Jovanovic (Erlangen), C. Kandzia (Aachen), M. Keßler (Stuttgart), T. Kier (Oberpfaffenhofen), M. Klaas (Aachen), A. Klein (München), I. Klioutchnikov (Aachen), M. Kloker (Stuttgart), J. Kokavecz (Göttingen), M. Konstantinov (Göttingen), E. Krämer (Stuttgart), H.-P. Kreplin (Göttingen), M. Kriegel (Berlin), A. Krumbein (Göttingen), M. Kruse (Braunschweig), F.-O. Lehmann (Rostock), T. Lerche (Hamburg), T. Lutz (Stuttgart), H. Mai (Göttingen), M. Meinke (Aachen), F. Menter (Otterfing), R. Meyer (Berlin), C. Mockett (Berlin), T. Möller (Braunschweig), D. Müller (Aachen), B. Müller (Berlin), C.-D. Munz (Stuttgart), A. Nemili (Aachen), W. Nitsche (Berlin), F. Obermeier (Freiberg), H. Olivier (Aachen), C. Othmer (Wolfsburg), I. Peltzer (Berlin), J. Raddatz (Braunschweig), R. Radespiel (Braunschweig), L. Reimer (Braunschweig), M. Rein (Göttingen), B. Reinartz (Aachen), C. Resagk (Ilmenau), S. Reuss (Göttingen), K. Richter (Göttingen), U. Rist (Stuttgart), M. Ritter (Göttingen), H. Rosemann (Göttingen), T. Rösgen (Zürich), C.-C. Rossow (Braunschweig), F. Rüdiger (Dresden), M. Rütten (Göttingen), E. Sarradj (Cottbus), M. Schmidt (Aachen), G. Schmitz (Hamburg), P. Scholz (Braunschweig), N. Schönwald (Berlin), W. Schröder (Aachen), E. Schülein (Göttingen), V. Schulz (Trier), J. Schumacher (Ilmenau), D. Schwamborn (Göttingen), T. Schwarz (Braunschweig), A. Seitz (Braunschweig), W. Send (Göttingen), M. Siebenborn (Trier), C. Stemmer (Garching), A. Stück (Braunschweig), A. Stuermer (Braunschweig), E. Stumpf (Aachen), F. Thiele (Berlin), C. Tropea (Darmstadt), C. Weckmüller (Berlin), W. Wegner (Göttingen), K. Weinman (Göttingen), M. Widhalm (Braunschweig), J. Wild (Braunschweig), C. Willert (Köln), and W. Würz (Stuttgart).

Nevertheless, the authors sign responsible for the contents of their contributions.

The editors are grateful to Prof. Dr. W. Schröder as the General Editor of the "Notes on Numerical Fluid Mechanics and Multidisciplinary Design" and to the Springer-Verlag for the opportunity to publish the results of the Symposium.

June 2013

A. Dillmann
G. Heller
E. Krämer
H.-P. Kreplin
U. Rist

Contents

Part XII Biofluid Mechanics

Part I
Airplane Aerodynamics

Influence of Meshing on Flow Simulation in the Wing-Body Junction of Transport Aircraft

Philipp Peter Gansel, Patriz Dürr, Markus Baumann, Thorsten Lutz and Ewald Krämer

Abstract A common problem in the field of CFD simulations of aircraft is the construction of hybrid grids at concave geometry corners. The challenge is to generate boundary layer meshes normal to both intersecting walls, while none of the grid cells collide with each other. Boundary layer interaction combined with pressure gradients and three-dimensional effects causes very complex flows which demand a high mesh quality. An unstructured and three different hybrid grids of a generic aircraft geometry are compared to each other. The analysis focuses on the results in the wing-body junction. With the smallest meshing effort the unstructured grid simulation yields good agreement of surface pressure and boundary layers with the hybrid meshes. The strong impact of the boundary layer grid edge on the velocity profiles emphasizes the need of sufficiently high boundary layer grids on all surface parts.

1 Introduction

Continuous progress is achieved in CFD simulations of industry-relevant aircraft configurations by the availability of new numerical methods and modeling as well as increasing computational capabilities. However the spatial discretization in terms of computational mesh is disregarded often. Especially when meshing entire

P. P. Gansel (✉) · P. Dürr · M. Baumann · T. Lutz · E. Krämer
Institute of Aerodynamics and Gas Dynamics, University of Stuttgart, Pfaffenwaldring 21, 70569 Stuttgart, Germany
e-mail: gansel@iag.unistuttgart.de|
http://www.iag.uni-stuttgart.de/

T. Lutz
e-mail: lutz@iag.uni-stuttgart.de

E. Krämer
e-mail: Kraemer@iag.uni-stuttgart.de

A. Dillmann et al. (eds.), *New Results in Numerical and Experimental Fluid Mechanics IX*, Notes on Numerical Fluid Mechanics and Multidisciplinary Design 124,
DOI: 10.1007/978-3-319-03158-3_1,

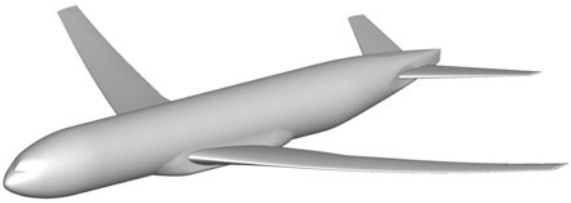

Fig. 1 NASA CRM including wing, body, belly fairing and horizontal tail plane

aircraft geometries with a variety of components and corners for viscous simulations problems occur with most grid generators using hybrid grids. The most frequent challenge in the vicinity of concave corners is to generate a boundary layer mesh normal to both intersecting walls, without having the grid cells collide with each other, which often leads to grids of locally poor quality. Actually the interaction of both boundary layers in combination with strong pressure gradients and three-dimensional effects causes very complex flows. Their simulation claims a high quality mesh and is challenging today's turbulence models.

Basic experimental and numerical investigations of the horseshoe vortex system developing at a wing-body junction have been conducted. The flow regime is also present in wind tunnel testing at the junction of the airfoil with the test section side walls. An overview of different measured and simulated geometries can be found in [1]. In simulations of the Reynolds-Averaged Navier-Stokes (RANS) equations the grid and turbulence model dependency of the corner separation is a known problem which presumably arises from the deficiency of eddy-viscosity models to represent the anisotropy of the Reynolds stresses (see e.g. [2]).

In the present study particularly the influence of the meshing strategy on the simulation of the junction flow is investigated to highlight the effects separately.

2 Simulation Setup

2.1 Test Case

The NASA Common Research Model (CRM), a representative commercial transport aircraft configuration (see [3]), is used as test case in this study. The generic geometry consists of a fuselage, a transonic wing, a belly fairing and a horizontal tail plane. The considered configuration in Fig. 1 omits the nacelle and pylon to provide a clean wing. The CRM has been subject to the Drag Prediction Workshops (DPW) IV and V, where different numerical results and comparisons of grid generators and flow solvers could be achieved (see [4]). Experimental wind tunnel results were published by NASA amongst others in [5].

The CFD model has a reference wing area of 383.690 m^2 and a mean aerodynamic chord of 7.005 m. The wing has a span of 58.763 m, an aspect ratio of 9.0 and a taper ratio of 0.275. The quarter chord line is swept back by 35°. The considered freestream

Table 1 Grid points and cell element counts of the used CFD meshes

Grid	Points	Tets	Prisms	Pyras	Hexas	Cells
GG aniso tets	13,530,358	80,375,105	–	–	–	80,375,105
GG recomb prisms	13,530,484	64,378,306	5,332,464	–	–	69,710,770
PW recomb prisms	13,530,358	19,164,798	20,389,639	20,695	–	39,575,132
GG hexa and prisms	10,189,056	11,495,105	5,520,872	70,186	5,357,947	22,444,110

conditions $Ma = 0.85$, $Re = 5 \cdot 10^6$ and $c_l = 0.5$ represent the CRM design point despite a lower Reynolds number ($Re_{\text{design}} = 40 \cdot 10^6$).

2.2 Grids

Basically there are three different meshing topologies: structured, unstructured and hybrid grids. Although structured grids have the big advantages of structured calculation schemes and proper resolution of corner flow boundary layers, the disadvantages of high generation effort and point numbers—unless methods like hanging nodes or overset grids are used—limit their applicability for complex geometries. One unstructured grid consisting of tetrahedra only and three different hybrid meshes are investigated in the present study. The total grid point and cell element counts are displayed in Table 1.

Unstructured Grid "GG Aniso Tets" Production, refinement and adaption of unstructured grids are very simple. Usually they consist of nearly isotropic tetrahedra, which mostly restricts possible applications to Euler or other simulations with no need of a boundary layer resolution. Such a RANS mesh would have an exhaustively high surface and near wall resolution caused by having the same cell size in tangential and wall normal direction. The grid generator used for the considered meshes Gridgen V15.18 [6] provides anisotropic tetrahedral elements to solve this problem. In the meshing process points of an unstructured surface mesh are extruded from the walls. The resulting prisms are divided into three tetrahedral each. This allows an adequately resolved boundary layer using element aspect ratios up to three orders of magnitude. After completing a prescribed amount of anisotropic element layers (in this case 35) the remaining flow domain is filled up with ordinary tetrahedra. Figure 2 illustrates the boundary layer resolution in the wing-body junction and near the wing leading edge of this mesh referenced as "GG aniso tets". In order to avoid grid cells to collapse or overlap with others the grid extrusion process is stopped in concave corner regions before it reaches the designated boundary layer mesh height. Another specific problem of this kind of unstructured mesh is an increased numerical error introduced by the extremely skewed tetrahedra. If a cell vertex scheme is used, the angles of some faces of the median dual grid, the fluxes are evaluated on, to the corresponding edge deviate extremely from the 90° optimum (see [7]).

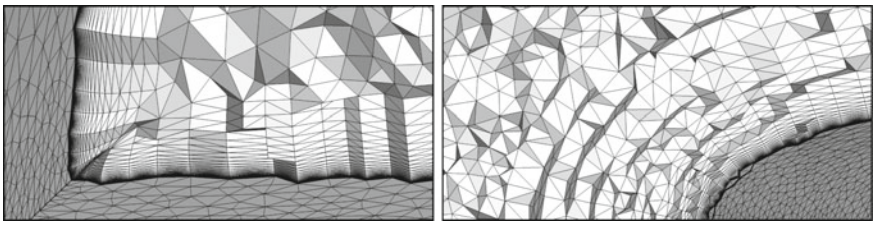

Fig. 2 Details of the "GG aniso tets" grid in the wing-body junction and near the wing leading edge

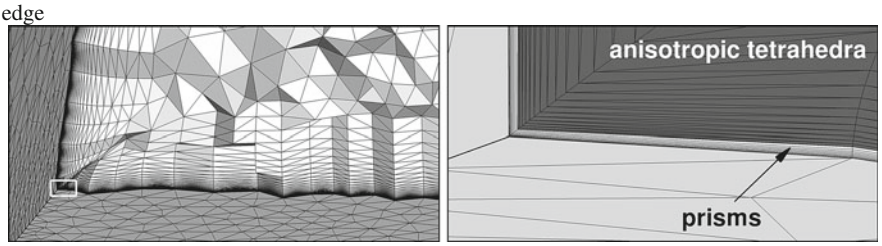

Fig. 3 Details of the "GG recomb prisms" grid in the wing-body junction

Hybrid Grid "GG Recomb Prisms" To prevent the accuracy issue of anisotropic unstructured elements Gridgen provides the possibility to recombine prisms of three anisotropic tetrahedra at a time in the boundary layer part of the grid. The required connectivity information is present in the mesh data from the cell extrusion process. The unstructured grid is divided in two blocks—one tetrahedral and one prismatic—which can be edited further individually. A strong constrain is that the new built prism block must consist of complete element layers. Because of the described chopping of extrusion layers in the vicinity of corners only few prisms layers can be constructed in this way. The grid "GG recomb prisms" which is derived from "GG aniso tets" using this functionality achieves 9 layers of prisms at the walls. They cover only a very thin part of the boundary layer mesh (see Fig. 3) which also explains the relatively small decrease of element count compared to the "GG aniso tets" mesh in Table 1.

Hybrid Grid "PW Recomb Prisms" The Gridgen succeeding meshing software Pointwise [8] provides another approach where all anisotropically extruded tetrahedra are used for prism recombination (up to 35 prism layers in this case). This can only be done at the very end of mesh generation with no further editing. In the current version V17.0R2 it is embedded in the export process of finished grids to the simulation software. To obtain a mesh suitable for the used CFD code TAU an appropriate export plugin for Pointwise had to be developed first. It outputs a TAU readable NetCDF mesh and includes the prisms recombination. The resulting grid is referenced as "PW recomb prisms". Figure 4 shows detailed views of the wing-body junction and the wing leading edge. Note that—originating from the same unstructured grid—"GG aniso tets", "GG recomb prisms" and "PW recomb prisms"

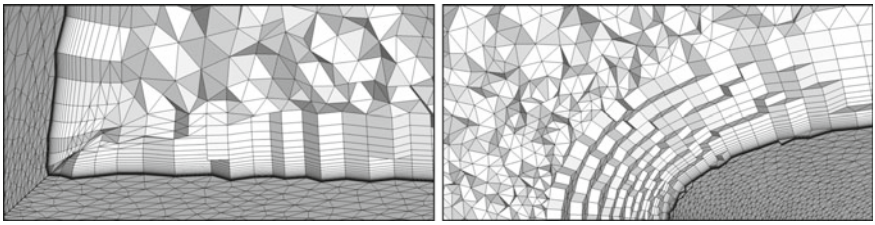

Fig. 4 Details of the "PW recomb prisms" grid in the wing-body junction and near the wing leading edge

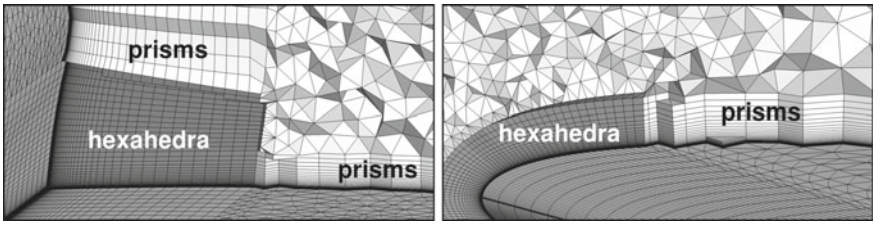

Fig. 5 Details of the "GG hexa and prisms" grid in the wing-body junction and near the wing leading edge

have identical surface meshes, outer region unstructured meshes and volume grid points.

Hybrid Grid "GG Hexa and Prisms" As any other hybrid grids where the boundary layer mesh is extruded from the surface the three grids described above suffer from deficient boundary layer resolution in two ways. Because of the chopping near geometry corners the boundary layer mesh there is too thin and the outer part of the boundary layer cannot be resolved by the outer isotropic tetrahedral mesh. The second aspect is the near wall resolution which close to the corner is defined by the surface mesh of the respectively other wall. This usually leads to a wall distance of the first point orders of magnitudes higher than desired. One possible solution to these problems is to adopt some aspects of structured meshing. By inserting volume blocks of hexahedral elements in the corners the boundary resolution normal to both walls can be ensured and adjusted independently. Such combinations of structured and hybrid meshing was already investigated mostly using chimera technique e.g. in [9] and [10]. In the present study the hexahedral and prismatic grid parts are connected to each other directly, which can be seen in Fig. 5. The hexahedral blocks are wrapped around the wing-body junction in an O-type topology. The leading/trailing edge and wingtip regions are meshed with hexahedra, too. This enables independent resolution in chord- and spanwise dierection, but does not affect the considered junction region. The remaining surface parts are filled up with prisms. The same is applied to the horizontal tail plane.

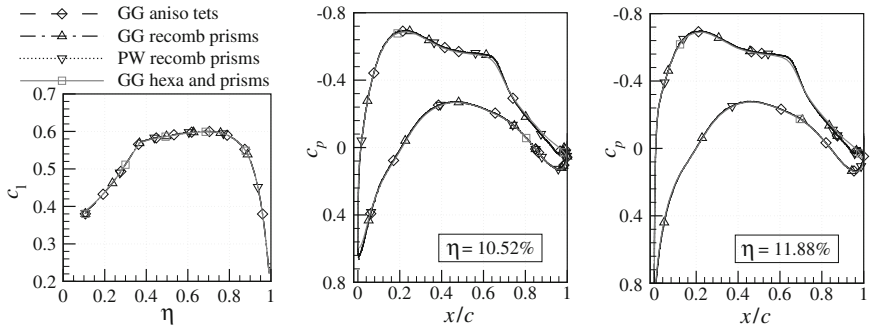

Fig. 6 Spanwise lift distribution on the different meshes (*left*) and streamwise pressure distribution at $\eta = 10.52\,\%$ (*middle*) and $11.88\,\%$ (*right*).

2.3 Numerics

The simulations are conducted using the unstructured finite volume code TAU (DLR) [11] in the versions 2011.2.0 and 2012.1.0. Central discretization scheme with artificial matrix dissipation is applied. Residual smoothing and a 3w+ multigrid cycle are used for convergence acceleration. To enable the usage of identical and low-dissipation parameters on all grids the one-equation turbulence model of Spalart and Allmaras [12] was applied due to its stability advantages over Reynolds stress models which also account for the turbulence anisotropy.

3 Results and Discussion

Despite the varying grid types the integral forces on all meshes agree very well. Differences in the spanwise c_l distribution (Fig. 6, left) are within one line width.

Remarkable differences of pressure distribution can be found in the area of the wing-body junction. While the results on the unstructured grid and the two derived hybrid grids yield the same c_p close to the corner in Fig. 6 (middle and right), the solution on the "GG hexa and prisms" grid shows slightly lower pressure close to the leading edge and a less pronounced separation at the trailing edge. The deviation in the area of the shock is due to an insufficient refinement of "GG hexa and prisms" on the wing upper surface. The wall normal velocity profiles of the boundary layer at $\eta = 10.52\,\%$ are plotted in Fig. 7 (upper row) for three streamwise positions. Due to the chopping of anisotropic or prismatic elements all grids except "GG hexa and prisms" show characteristic kinks in the velocity profiles at the border to the outer flow grid's isotropic tetrahedra at $20\,\%$ and $40\,\%$ chord length. "GG hexa and prisms" produces a smooth velocity profile and reaches the outer boundary layer edge velocity at a higher wall distance. At $98\,\%$ a much smaller separation is evident on the hexahedral cells. In the lower row of Fig. 7 there are only small differences

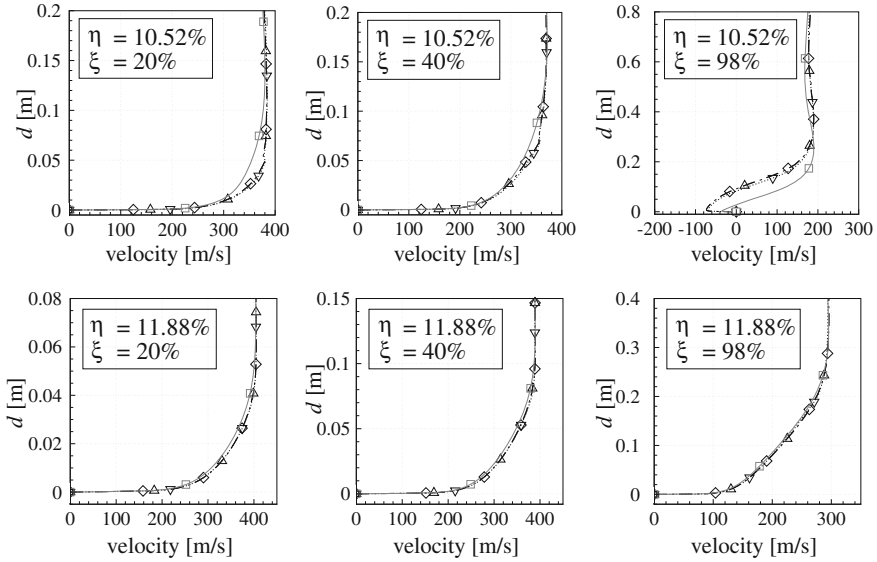

Fig. 7 Boundary layer velocity profiles at two spanwise and three streamwise positions. The same line legend applies as in Fig. 6

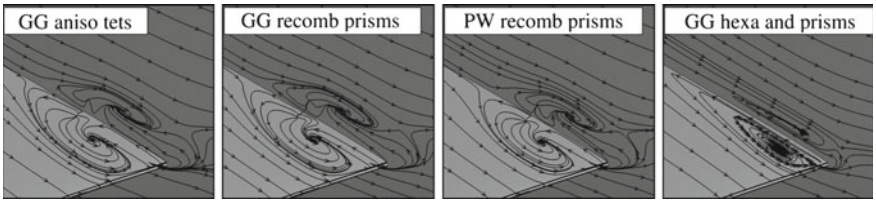

Fig. 8 Wall shear stress lines at the trailing edge of the wing-body junction

in the velocity profiles at $\eta = 11.88\,\%$, although small kinks on the first three meshes remain visible. No trailing edge separation is predicted at this spanwise location.

Looking closer at the corner separation at the trailing edge of the wing-body junction in Fig. 8 all grids based on the "GG aniso tets" grid predict the same shape and dimensions (6.5 % chord streamwise and 1.0 % half span spanwise). On the "GG hexa and prisms" grid the separation is longer (9.3 %), slightly narrower (0.8 %) and also lower as indicated by the flatter streamline swirl on the fuselage. The appearance of the corner separation is under discussion and already found in previous numerical simulations of the CRM (e.g. in [4]).

Also the pressure differences at the leading edge of "GG hexa and prisms" grid can be explained by the better boundary layer discretization using hexahedral cells. Figure 9 shows the differences in resulting flow topologies on "PW recomb prisms" and "GG hexa and prisms". On the prismatic mesh the streamlines just follow the

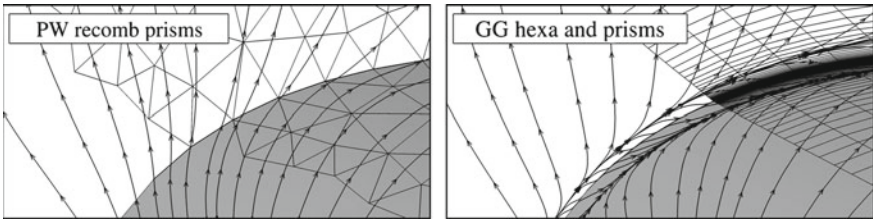

Fig. 9 Wall shear stress lines at the leading edge of the wing-body junction

induction of the developing horseshoe vortex and run from the wing over the corner to the fuselage surface. The higher resolution of the hexahedral grid in contrast can reproduce their separation close to the corner and reattachment at the fuselage. Thus a counter-rotating secondary vortex is formed in the wing-body junction. Even with refined surface triangles the prismatic volume mesh would still suffer from an even stronger reduction of the boundary layer grid height and the consequential kinks in the velocity profiles.

4 Conclusions

The all tetrahedral unstructured mesh—which is the way fastest to generate—yields results comparable to the usual prismatic hybrid grids in terms of integral forces, pressure distribution and boundary layer data including separation prediction. However all of these meshes show a strong effect on the boundary layer profile when the border of anisotropic or prismatic cells is shifted towards the surface inside the boundary layer. This is the case at the wing-body junction, where only the grid with hexahedral cells in the corner can resolve the complete boundary layer. This also results in another secondary flow topology very close to the corner and differences in the prediction of trailing edge separation.

References

1. Gand, F., Deck, S., Brunet, V., Sagaut, P.: Flow dynamics past a simplified wing body junction. Phys. Fluids **22**, 115111 (2010)
2. Klein, A., Illi, S., Nübler, K., Lutz, T., Krämer, E.: Wall Effects and Corner Separations for Subsonic and Transonic Flow Regimes. In: Kroener, D.B., Resch, M.M. (eds.) High Performance Computing in Science and Engineering '11, pp. 393–407. Springer, Berlin (2011)
3. Vassberg, J.C., DeHaan, M.A., Rivers, S.M., Wahls, R.A.: Development of a Common Research Model for Applied CFD Validation, Studies. AIAA-2008-6919 (2008)
4. Vassberg, J.C., Tinoco, E.N., Mani, M., Rider, B.: Summary of the Fourth AIAA CFD Drag Prediction Workshop. AIAA 2010–4547 (2010)
5. Rivers, M.B., Dittberner, A.: Experimental Investigations of the NASA Common Research Model in the NASA Langley National Transonic Facility and NASA Ames 11-Ft Transonic Wind Tunnel. AIAA 2011–1126 (2011)

6. Pointwise, Inc.: Gridgen Version 15. User Manual, Fort Worth (2012)
7. Aftonis, M., Gaitonde, D., Tavares, T.S.: Behaviour of linear reconstruction techniques on unstructured meshes. AIAA J. **33**(11), 2038–2049 (1995)
8. Pointwise, Inc.: Pointwise User Manual, Fort Worth (2012)
9. Doerffer, P., Szulc, O.: High-lift behaviour of half-models at flight reynolds numbers. Task Quart. **10**(2), 191–206 (2006)
10. Crippa, S.: Application of novel hybrid mesh generation methodologies for improved unstructured CFD simulations. AIAA 2010–4672 (2010)
11. Schwamborn, D., Gerhold, T., Heinrich, R.: The DLR TAU-code: recent applications in research and industry. In: ECCOMAS, Egmond a.Z., (2006)
12. Spalart, P.R., Allmaras, S.R.: A one-equation turbulence model for aerodynamic flows. AIAA-92-0439 (1992)

Numerical Approach Aspects for the Investigation of the Longitudinal Static Stability of a Transport Aircraft with Circulation Control

Dennis Keller

Abstract The aim of the investigation is to gain more certainty about the approach to evaluate the longitudinal stability and controllability of a high-lift configuration of a transport aircraft with circulation control. Since the work was carried out with a CFD RANS approach, a comprehensive meshing study was performed in advance.

1 Introduction

In compliance with the vision *Flightpath 2050*, the German research project *SFB 880* is investigating a STOL aircraft configuration, which possibly allows to reduce emissions and travel time by utilizing existing aerospace infrastructure more efficiently. In order to achieve short runway usage, an active high-lift system in terms of circulation control (CC) is employed. The potential of such systems is already well known (see [5, 8]) and is further assessed within the research project by M. Burnazzi [2]. However, the technology raises new questions, which are not adequately addressed so far. One of those is how CC will impact the handling qualities of a transport aircraft. For example, it is expected that the high flap loading and the low dynamic pressure during take off and landing will pose challenges to the flight control systems. This paper gives an aerodynamic view of the longitudinal static stability issue by investigating the flight mechanical properties of a circulation controlled wing itself, its influence on the HTP and eventually of the whole aircraft. Prior to the analysis, a meshing study was performed on a simplified 2D geometry in order to derive an efficient and accurate meshing strategy for the 3D configuration.

D. Keller (✉)
Institute of Aerodynamics and Flow Technology, German Aerospace Center,
38108 Braunschweig, Germany
e-mail: Dennis.Keller@dlr.de

A. Dillmann et al. (eds.), *New Results in Numerical and Experimental Fluid Mechanics IX*,
Notes on Numerical Fluid Mechanics and Multidisciplinary Design 124,
DOI: 10.1007/978-3-319-03158-3_2,

Table 1 Number of grid points

	Coarse	Medium	Fine
Structured	128454	524558	2119854
Hybrid_PW	–	284918	–
Hybrid	84856	181714	337342

2 Flow Solver

The calculations are performed with the *DLR TAU* code [6], which is based on an unstructured finite volume approach for solving the Reynolds-averaged Navier Stokes equations. For this investigation, the implicit LUSGS scheme is used for time stepping and a central scheme for the spatial discretization of the convective fluxes. The turbulence effects are modeled with the original Spalart-Allmaras formulation (SA) [12] with vortical and rotational flow correction based on the Spalart-Shur correction [13].

3 Test Configurations

3.1 2D Configuration

The 2D geometry represents a cut through the wing of the reference aircraft at the location of its mean aerodynamic chord. In order to investigate discretization influences especially near the active flow outlet, several cell size settings as well as different meshing methods were utilized (Table 1). Hybrid meshes were created with Pointwise [10] (Hybrid_PW) and Centaur [3] (Hybrid), whereas structured meshes were solely built with the former (Structured) (Fig. 1). The edge lengths along the surface were kept almost equal within the refinement levels. However, small adaptions had to be introduced on the Centaur meshes in order to achieve an optimal boundary layer discretization. Furthermore, in contrast to the structured meshes, the wall distances of the quad layers were kept constant on these meshes.

3.2 3D Configuration

At the beginning of the *SFB 880* research project, an aircraft with a capacity of 100 passengers was designed with the preliminary aircraft design tool *PrADO* [7]. The wing's span measures 28.8 m with an aspect ratio of 9 and a leading edge sweep of 10°. The HTP's span equals 10.4 m, resulting in a relative tail volume of 1.235. The underlying 3D geometry (Fig. 5) represents the landing configuration of this design,

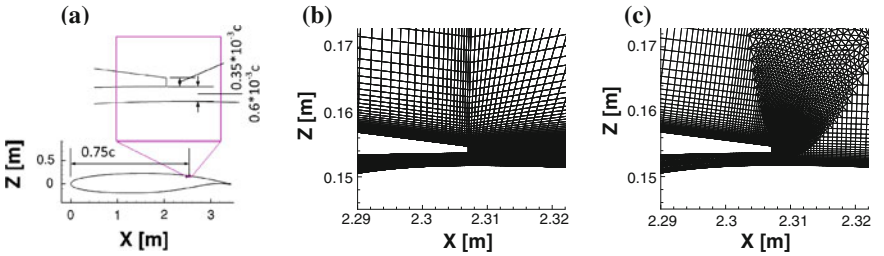

Fig. 1 Slot region. **a** Geometry. **b** Structured mesh. **c** Hybrid mesh

which has no leading edge device but a circulation controlled plain flap and aileron with 65° deflection and 45° droop, respectively. Hybrid meshes were built for the tail-off configuration and for the whole aircraft based on the experiences from the 2D investigations. The wing wake was refined with either tetrahedra or with a structured hexahedron box. A modular mesh approach was chosen in order to trim the aircraft with the smallest possible meshing influence.

4 Computational Results

4.1 Preliminary 2D Studies

Grid Convergence Study When working with complex geometries, semi automated hybrid mesh generators often seem to be the best choice as they offer a good compromise between work effort and quality of results. However, the quality may become unacceptable low when the automated mesh topology does not reflect the flow topology. Typical examples for this are free shear layers. With the investigation of wake interaction and CC in general, these types of flow phenomena are of particular importance. Therefore, the main purpose of the meshing study was to evaluate the feasibility of using a semi automated hybrid mesh generator for these kind of problems. Furthermore, a grid convergence study was carried out for both the structured as well as the hybrid mesh approach.

Figure 2 shows the influence of the grid resolution on the global coefficients for both mesh families. While the coefficients of the structured mesh show a clear trend, the hybrid meshes have a change in gradients at the medium size mesh. However, when considering the difference in grid sizes, the hybrid meshes deliver good results. Following G. de Vahl Davis [4] and applying the Richardson Extrapolation on the structured mesh family, the *exact* coefficients and the deviations of the medium sized meshes can be derived [11]. With far less than one per cent in deviation from the *exact* lift and moment coefficients, both medium size meshes show excellent results (Table 2). The comparably high difference in drag is probably coming from small

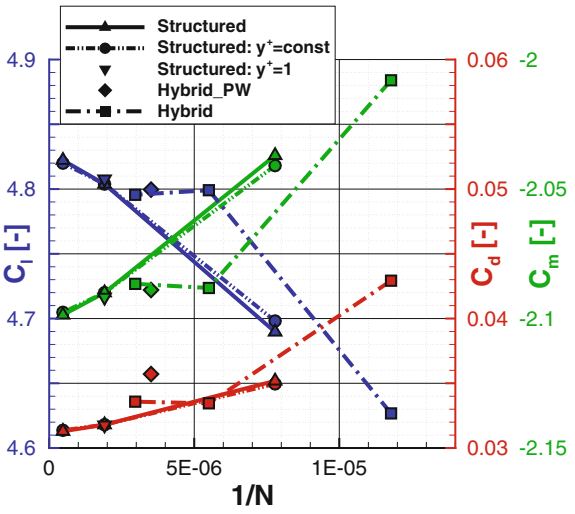

Fig. 2 Grid dependence of global coefficients

Table 2 Error estimates for global coefficients

	Coarse		Medium			Fine	
	Structured	Hybrid	Structured	Hybrid_PW	Hybrid	Structured	Hybrid
$\frac{c_l - c_{l,R.ex.}}{c_{l,R.ex.}}$ [%]	2.82	4.12	0.455	0.54	0.56	0.073	0.625
$\frac{c_d - c_{d,R.ex.}}{c_{d,R.ex.}}$ [%]	12.77	37.58	1.93	14.46	7.12	0.31	7.63
$\frac{c_m - c_{m,R.ex.}}{c_{m,R.ex.}}$ [%]	3.01	4.39	0.488	0.54	0.57	0.079	0.65

pressure differences on the flap, which have a large influence on the drag coefficient due to its order of magnitude.

The pressure distribution supports this assumption (Fig. 3). While showing only slight differences in most parts, the suction peak on the coanda surface indicates a bigger impact by the discretization level. It also reflects the change in gradients of the global coefficients of the hybrid mesh family, with the peak being stronger on the medium hybrid mesh than the one on the fine hybrid mesh.

The velocity profiles within the boundary layer show a fairly good agreement for the medium and fine meshes in all investigated cuts except at the slot exit (Fig. 4). Here, the velocity within the slot seems to be overestimated on all hybrid Centaur meshes. Furthermore, the velocity distributions on the coarse and the medium hybrid mesh show a peak towards the upper wing surface. Comparison to experimental investigations of circulation controlled airfoils [1, 9] lead to the assumption, that these peaks are unphysical and arise due to the O-type topology at the wing trailing edge. In contrast, the velocity profiles on all structured meshes show a homogeneous distribution. However, the higher velocities at the slot exit on the hybrid meshes do not seem to have a big influence on the general flow topology, since this difference cannot be detected in the velocity distributions further downstream anymore.